Periodically poled lithium niobate waveguide sum-frequency generator for efficient single-photon detection at communication wavelengths

Rostislav V. Roussev, Carsten Langrock, Jonathan R. Kurz, and M. M. Fejer

Edward L. Ginzton Laboratory, Stanford University, Stanford, California 94305-4085

Received November 24, 2003

We present a device to facilitate single-photon detection at communication wavelengths based on continuous-wave sum-frequency generation with an upconversion efficiency exceeding 90%. Sum-frequency generation in a periodically poled lithium niobate waveguide is used to upconvert signal photons to the near infrared, where detection can be performed efficiently by use of silicon avalanche photodiodes.

OCIS codes: 270.5570, 190.2620, 190.7220, 130.3120, 040.3060.

Single-photon detection at wavelengths in the fiber-optic communications band[1,2] is important for quantum-optics applications, such as quantum cryptography. High detection efficiency near 1.55 μm permits compatibility with existing fiber-optics technology in which fiber losses are minimized. Current detection devices operating at these wavelengths cannot deliver the performance needed to implement, for example, quantum key distribution as required by the BBM92 quantum coding scheme[3] over distances longer than a few tens of kilometers because of limitations imposed by high dark counts and low detection efficiencies. Two of the more prominent devices currently used are InGaAs–InP avalanche photodiodes (APDs) and solid-state photomultipliers. Both suffer from low quantum efficiency[4] (QE) ($<16\%$ at 1.3 μm and $<7\%$ at 1.55 μm) and high dark counts ($>10^4$–10^5/s). Furthermore, the operation of either of these devices requires liquid-nitrogen cooling. In contrast, single-photon detection in the near-infrared (NIR; 600–800 nm) can be performed efficiently with silicon APDs. Single-photon counting modules (SPCMs) with detection efficiencies in the range 50–70% with dark counts below 25/s are commercially available. Improved detection has been reported with quantum efficiencies in excess of 75% at 700 nm.[5] Silicon-APD-based SPCMs require only the moderate cooling that is provided by an integrated thermoelectric element. One can take advantage of these detectors if efficient conversion from 1.55 μm to the NIR is available.

Frequency upconversion of weak signals is possible by sum-frequency generation (SFG) with a stronger pump wave. Single-photon detection with SFG requires low insertion loss of the upconversion device as well as isolation of the converted photons from the parasitic second harmonic (SH) of the pump to prevent adding of false counts. In addition, high conversion efficiency can help to reduce the pump power requirement and the unacceptable pump SH. Single-photon detection of 1.55-μm photons by means of frequency upconversion in bulk periodically poled lithium niobate (PPLN) was recently demonstrated.[6] This detection scheme relied on efficient conversion of photons, by use of a 1.06-μm pump, from the *C* band to 630 nm in a ring cavity, where they were detected by a SPCM. The 100-nm separation between the upconverted signal and the pump SH allowed adequate discrimination to be made between the two. The overall detection efficiency was 55% at 20 W of circulating pump power. We propose to implement upconversion in a waveguide that offers the convenience of a monolithic fiber-pigtailed device, nonresonant single-pass operation, and moderate pump power requirement.

For efficient conversion in nonlinear optical frequency mixing, high field intensities and long interaction lengths are necessary, both of which can be achieved simultaneously in a guided-wave structure. SFG in PPLN waveguides was used previously to produce low-power all-optical gates[7] and optical sampling systems.[8] Although these devices had high mixing efficiencies, they could not be applied to photon counting, as the demands for this application emphasize several properties that are less important in other signal processing applications. In particular, high-QE counting requires low passive insertion loss and ease of separation of the desired sum-frequency signal from the more intense parasitic SHG of the pump favors a large separation of the signal and the pump wavelengths (for example, 1.55 and 1.32 μm). The annealed proton exchanged waveguides used in the previous experiments are not easily adapted to meet these demands, because their asymmetric refractive-index profile does not permit the implementation of tapers suitable for low-loss fiber pigtailing simultaneously at the two input wavelengths.

For these reasons we chose to implement the SFG devices for the photon counting application by using the recently developed reverse proton exchange (RPE) process.[9,10] These waveguides are characterized by a refractive-index profile that is symmetric in depth and by the highest conversion efficiency reported to date,[11] three times larger than in annealed proton exchanged waveguides. The symmetric refractive-index profile permits the design of waveguides that are single

0146-9592/04/131518-03$15.00/0

mode over a wide wavelength range. Single-mode RPE waveguides in the range 1.06–1.6 μm with propagation losses as low as 0.1 dB/cm have been demonstrated.[12]

The theory of three-wave mixing in waveguides is mathematically equivalent to a plane-wave interaction and permits complete energy conversion from one wavelength to another.[13] For SFG the electric fields of the signal (E_1), the pump (E_2), and the sum-frequency wave (E_3) can be written as $E_i(x, y, z) = A_i(z)E_i(x, y)\exp(-j\beta_i z)$, where $i \in \{1, 2, 3\}$, $E_i(x, y)$ are the normalized modal electric fields, $A_i(z)$ is the amplitude of the ith mode, and $\omega_3 = \omega_1 + \omega_2$. The evolution of envelopes A_i follows the coupled-mode equations

$$\frac{\mathrm{d}A_1}{\mathrm{d}z} = -j\kappa_1\nu^* A_2{}^* A_3 \exp(-j\Delta\beta z) - \frac{\alpha_1}{2} A_1, \quad (1a)$$

$$\frac{\mathrm{d}A_2}{\mathrm{d}z} = -j\kappa_2\nu^* A_1{}^* A_3 \exp(-j\Delta\beta z) - \frac{\alpha_2}{2} A_2, \quad (1b)$$

$$\frac{\mathrm{d}A_3}{\mathrm{d}z} = -j\kappa_3\nu A_1 A_2 \exp(j\Delta\beta z) - \frac{\alpha_3}{2} A_3, \quad (1c)$$

with the coupling coefficients and the phase mismatch defined as

$$\kappa_i = \left(\frac{8\pi^2 d_{\mathrm{eff}}{}^2}{n_1 n_2 n_3 c \epsilon_0 \lambda_i{}^2}\right)^{1/2}, \qquad \Delta\beta = \beta_3 - \beta_2 - \beta_1, \quad (2)$$

respectively, where d_{eff} is the effective nonlinear coefficient; n_i and α_i are the refractive index and the power attenuation coefficient, respectively, at wavelength λ_i; c is the vacuum speed of light; and ϵ_0 is the permittivity of free space. Wave vectors $\beta_i = 2\pi n_i/\lambda_i$ are defined as usual, and ν is the spatial overlap factor. For a first-order quasi-phase-matched grating and z-polarized modes, the effective nonlinear coefficient d_{eff} is given by $d_{\mathrm{eff}} = (2d_{33}/\pi)\sin(\pi D)$, where D is the poling duty cycle.

For an undepleted pump (i.e., $\mathrm{d}A_2/\mathrm{d}z = 0$) and negligible propagation losses (i.e., $\alpha_i = 0$), Eqs. (1) can be solved analytically. Applying the following boundary conditions and assuming zero phase mismatch (i.e., $\Delta\beta = 0$):

$$A_1(0) = \sqrt{P_{\mathrm{sig}}(0)}, \qquad A_2(0) = \sqrt{P_{\mathrm{pump}}}, \qquad A_3(0) = 0$$

yield the solution

$$N_{\mathrm{SFG}}(L) = N_{\mathrm{sig}}(0)\sin^2[(\eta_{\mathrm{nor}}P_{\mathrm{pump}})^{1/2}L], \quad (3a)$$

$$1 - \eta_{\mathrm{NL}} \equiv \frac{N_{\mathrm{sig}}(L, P_{\mathrm{pump}} > 0)}{N_{\mathrm{sig}}(L, P_{\mathrm{pump}} = 0)} = \cos^2[(\eta_{\mathrm{nor}}P_{\mathrm{pump}})^{1/2}L], \quad (3b)$$

where $N_i = |A_i|^2/(\hbar\omega_i)$ represent the photon numbers and $\eta_{\mathrm{nor}} \equiv \nu^2\kappa_1\kappa_3$ is the normalized power efficiency in the low-gain limit. In the absence of propagation losses, conversion efficiency η_{NL} introduced above is equal to the internal QE of the device, $N_{\mathrm{SFG}}(L)/N_{\mathrm{sig}}(0)$. Complete wavelength conversion is achieved when $P_{\mathrm{pump}} = P_{\mathrm{max}} = \pi^4/(4\eta_{\mathrm{nor}}L^2)$. Here the overall detection efficiency equals the efficiency of the NIR detector.

Assuming equal propagation losses (α) at the signal and SFG wavelengths, the overall detection efficiency, including the effects both of loss and of the finite detector quantum efficiency, can be expressed as

$$\eta_{\mathrm{tot}} = \eta_{\mathrm{NIR}}\eta_{\mathrm{NL}}\tau, \quad (4)$$

where η_{NIR} is the quantum efficiency of the NIR detector, η_{NL} is the level of signal depletion measured at the output, and $\tau = T_{\mathrm{in}}{}^{\mathrm{sig}}\exp(-\alpha L)T_{\mathrm{out}}{}^{\mathrm{SFG}}$ is the passive signal power transmission through the waveguide of length L. This transmission, which ideally is unity, is reduced by the nonunity coupling ($T_{\mathrm{in}}{}^{\mathrm{sig}}$) of the signal at the input by Fresnel reflections and modal mismatch and at the output by Fresnel reflections ($T_{\mathrm{out}}{}^{\mathrm{SFG}}$) at the sum frequency and by the propagation losses.

Our experimental setup for wavelength conversion is shown in Fig. 1. An external-cavity tunable diode laser (ECDL) at 1551 nm followed by an erbium-doped fiber amplifier (EDFA) is used as the pump source. The signal at 1340 nm is provided by a second ECDL. Note that the same device will work equally well with the roles of pump and signal reversed, as we intend to demonstrate in a future experiment. A dichroic mirror and a prism at the output of the chip are used to separate the SFG, the signal, and the pump. We used a Newport 1830C powermeter to measure the pump power after the chip and to calibrate the two optical spectrum analyzers, (OSAs), which we used to detect the residual signal and the SFG.

The wavelength conversion was performed in a RPE PPLN waveguide. The 4.8-cm-long PPLN chip was proton exchanged in benzoic acid at 171 °C for 24 h to a depth of 1.22 μm. After the chip was annealed in air at 312 °C for 23 h, it was reverse exchanged[11] at 300 °C for 30.6 h. A 2-mm-long 3.5-μm-wide (on the photolithographic mask) single-mode waveguide (mode filter) was included as the input section of the device to mode match a single-mode fiber input, followed by a 2-mm-long linear taper, increasing the waveguide width from 3.5 to 7 μm. Note that, because of the concentration-dependent

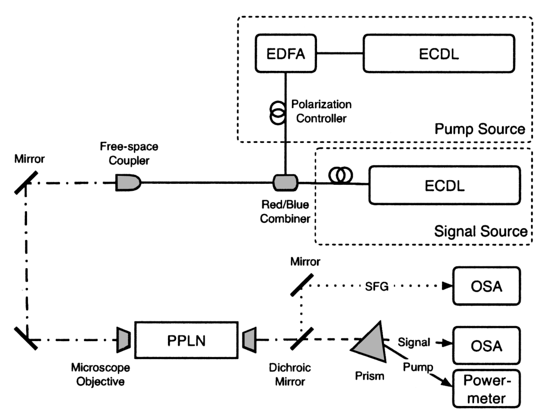

Fig. 1. Experimental setup for SFG of a 1.5-μm signal and a 1.3-μm pump.

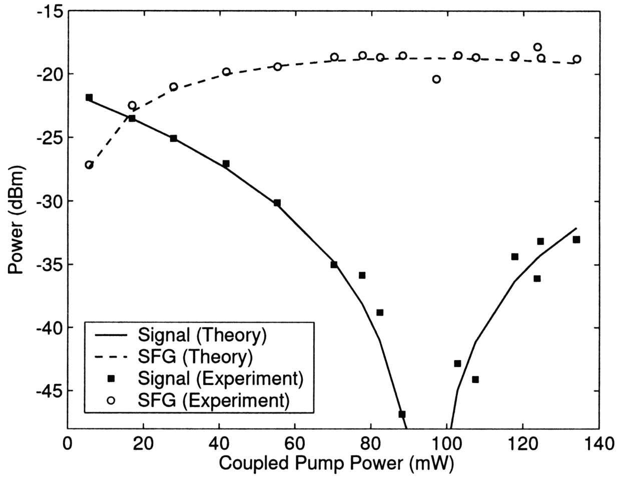

Fig. 2. Experimental and theoretical results obtained by numerical integration of coupled-mode equations (1); $\eta_{\mathrm{nor}} = 330\%/\mathrm{W\,cm}^2$, $\alpha_1 = \alpha_2 = \alpha_3 = 0.18$ dB/cm, $\lambda_{\mathrm{sig}} = 1.34\ \mu\mathrm{m}$, $\lambda_{\mathrm{SFG}} = 0.719\ \mu\mathrm{m}$, $L = 4$ cm, and $P_{\mathrm{sig}} = 8.42\ \mu\mathrm{W}$.

diffusivity of protons in lithium niobate,[14] the mode size is (counterintuitively) smaller in the waveguides diffused through the wider mask sections. The length of the periodically poled 7-μm-wide interaction section was 40 mm. The device ended with a taper and a mode filter identical to the input taper and filter. The waveguide under test had propagation losses of 0.18 dB/cm at 1.35 and 1.55 μm as measured by the Fabry–Perot fringe-contrast method.[15] This method requires single-mode mode filters at the test wavelength, which precluded accurate measurement of the loss in the NIR. Independent SHG measurements of similar waveguides indicate that the losses in the NIR are comparable with the losses in the *C* band ($\alpha_{\mathrm{NIR}} \lesssim 2\alpha_{1.55\ \mu\mathrm{m}}$).

The normalized internal SFG efficiency was 330 ± 10%/W cm^2. The poling duty cycle was 37 ± 2%, reducing η_{nor} (and thus increasing $P_{\max}$) by 10–20% compared to that which would have been obtained with a 50% duty cycle. Signal depletion exceeding 99% was observed at 88 mW of pump power coupled into the waveguide (Fig. 2).

The overall internal quantum efficiency of our device is ~82% and is currently limited only by the propagation losses at the signal and sum wavelengths mentioned above. Taking the free-space-to-waveguide coupling efficiency of the signal into account as well as Fresnel reflections off of the end facets of the device, the external QE is 55%. The reduction in QE is caused mainly by Fresnel reflections for the signal at the input and the sum frequency at the output of the uncoated chip, each of which amounts to 13%. Antireflection coating the end facets will increase the external QE significantly. Free-space-to-waveguide mode-matching and fiber pigtailing losses of <0.5 dB each have been achieved and could be further reduced by improvements in the design and fabrication of the waveguide input taper. Without these anticipated improvements, the overall detection efficiency is approximately 41%, assuming a silicon APD with a QE of 75%. We anticipate demonstrating external upconversion efficiencies exceeding 80% and overall detection efficiencies exceeding 60%, with antireflection coatings and improvements in waveguide designs. Optimizing the poling duty cycle will reduce the pump power requirements by as much as 20%.

This work was supported by the Multidisciplinary University Research Initiative Center for Quantum Information Systems (Army Research Office/ Advanced Research and Development Agency program DAAD19-03-1-0199),the U.S. Air Force Office of Scientific Research under grant F49620-02-1-0240, the Defense Advanced Research Projects Agency through the University of New Mexico Optoelectronic Materials Research Center (DARPA Prime MDA972-00-1-0024), the Collaborative Research Program on Optical Signal Processing at Stanford University, and Crystal Technology, Inc. R. V. Roussev's e-mail address is rrousev@stanford.edu.

References

1. A. Karlsson, M. Bourennane, G. Ribordy, H. Zbinden, J. Brendel, J. Rarity, and P. Tapster, IEEE Circuits Devices Mag. **15,** 34 (1999).
2. M. Bourennane, A. Karlsson, J. P. Ciscar, and M. Mathés, J. Mod. Opt. **48,** 1983 (2001).
3. C. H. Bennett, G. Brassard, and N. D. Mermin, Phys. Rev. Lett. **68,** 557 (1992).
4. G. Ribordy, J.-D. Gautier, H. Zbinden, and N. Gisin, Appl. Opt. **37,** 2272 (1998).
5. P. G. Kwiat, A. M. Steinberg, R. Y. Chiao, P. H. Eberhard, and M. D. Petroff, Appl. Opt. **33,** 1844 (1994).
6. M. A. Albota and F. N. C. Wong, in *Conference on Lasers and Electro-Optics (CLEO)*, Vol. 88 of OSA Trends in Optics and Photonics Series (Optical Society of America, Washington, D.C., 2003), paper QThPDB11.
7. K. R. Parameswaran, M. Fujimura, M. H. Chou, and M. M. Fejer, IEEE Photon. Technol. Lett. **12,** 656 (2000).
8. T. Suhara, H. Ishizuki, M. Fujimura, and H. Nishihara, IEEE Photon. Technol. Lett. **11,** 1027 (1999).
9. J. Jackel and J. Johnson, Electron. Lett. **27,** 1360 (1991).
10. Y. Korkishko, V. Fedorov, T. Morozova, F. Caccavale, F. Gonella, and F. Segato, J. Opt. Soc. Am. A **15,** 1823 (1998).
11. K. R. Parameswaran, R. K. Route, J. R. Kurz, R. V. Roussev, M. M. Fejer, and M. Fujimura, Opt. Lett. **27,** 179 (2002).
12. R. Roussev, A. Sridharan, K. Urbanek, R. Byer, and M. Fejer, in *2003 IEEE LEOS Annual Meeting Conference* (Institute of Electrical and Electronics Engineers, Piscataway, N.J., 2003), Vol. 1, pp. 334–335.
13. K. R. Parameswaran, J. R. Kurz, R. V. Roussev, and M. M. Fejer, Opt. Lett. **27,** 43 (2002).
14. R. Roussev, X. Xie, K. Parameswaran, M. Fejer, and J. Tian, in *2003 IEEE LEOS Annual Meeting Conference* (Institute of Electrical and Electronics Engineers, Piscataway, N.J., 2003), Vol. 1, pp. 338–339.
15. R. Regener and W. Sohler, Appl. Phys. B **36,** 143 (1985).